Polymer Chemistry

Accepted Manuscript

This article can be cited before page numbers have been issued, to do this please use: M. G. Moloney, X. Liu and K. Okuda, *Polym. Chem.*, 2025, DOI: 10.1039/D4PY01474J.

ROYAL SOCIETY OF CHEMISTRY

rsc.li/polymers

View Article Online
DOI: 10.1039/D4PY01474J

ARTICLE

Polymerization Behavior of Biscarbenes Derived by Thermolysis of Bisdiazo Compounds

Received 00th January 20xx,
Accepted 00th January 20xx

DOI: 10.1039/x0xx00000x

Xiaosong Liu, [a] Mark G. Moloney* [a, b] and Koji Okuda [c]

ABSTRACT: A study of the collapse of bisdiazo compounds with different terminal groups upon heating, to generate reactive biscarbene intermediates has provided evidence for homopolymerization, in a process which proceeds in the absence of catalysts and is tolerant of oxygen. This polymerization behavior was monitored spectroscopically through UV-Vis kinetic analysis with various combinations of temperature and solvent, and clear evidence for dimer and trimer formation was found by Field Desorption Mass Spectrometry. Oligomerisation may involve the formation of C=C and C=N-N=C linkage, as studied validified by molecular dynamic (MD) calculations, before reaching macromolecular size. In the presence of terminal NH_2 groups, cross-linking resulting from carbene insertion, is also observed. This unusual polymerization of diazo monomers, when conducted on a polyvinyl alcohol (PVA) surface in the open-air upon heating, creates a highly crosslinked structure which changes surface properties.

Introduction

Diazo and bisdiazo compounds may react upon heating or activation by UV light, releasing nitrogen gas to generate highly active carbenes or biscarbenes intermediates. While they have been used successfully in polymer surface modification,[1, 2] they are more widely known for carbene insertion[3, 4] and coupling reactions.[5, 6] Diaryldiazo compounds tend to be oils or low melting solids,[7, 8] which are indefinitely stable while chilled but decompose on heating with an exotherm.[9] Of interest is that related bis(diaryldiazo) compounds are much more stable, more convenient to use and reactive under thermal conditions, offering a convenient platform for polymer surface modification reactions.[10] While polymerisation of radicals, as single electron species, are very well known (**Scheme 1a**), as are insertion and addition (**Scheme 1b**) reactions of carbenes, carbenic C1 polymerisations[11-13] have only more recently been developed (**Scheme 1c**), usually in the presence of metal catalysts[14]. A further development of carbene reactivity involving the oligomerisation and homopolymerization of biscarbenes induced by thermal decomposition of bisdiazo compounds is reported here, which can be acheived without using any catalyst (**Scheme 1d**), and even under aerobic conditions. In this work, using a combination of experimental and theoretical methods, several aspects have been investigated, beginning with a study of the rate of collapse of bisdiazo compounds under thermal conditions, followed by a study of the possible dimerization, oligomerization or polymerization processes which could be achieved without any catalyst in both solid- and liquid-phase, and lastly the identity of the possible oligomeric and polymeric products formed by such self-reaction and in particular the nature of the monomer linkages.

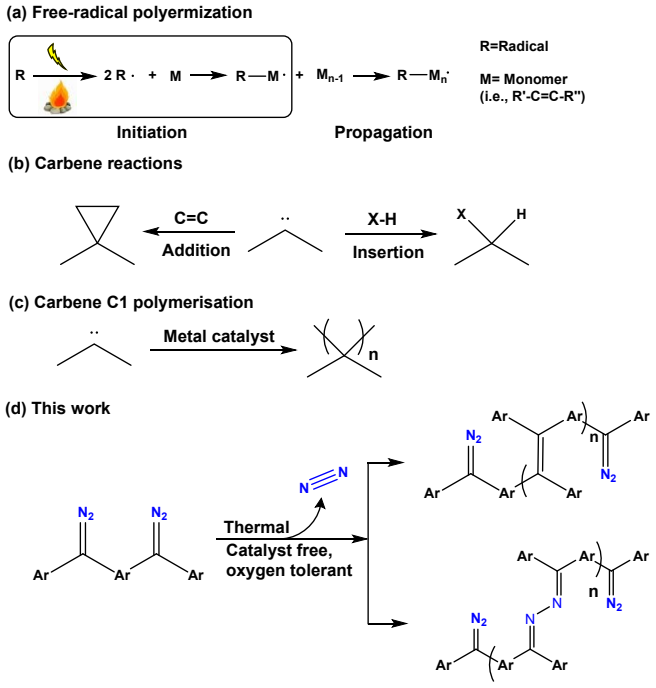

Scheme 1. Mechanism of (a) free-radical polymerization, (b) carbene reactions and (c) C1 polymerization, and (d) the catalyst-free polymerization from bisdiazo compounds as precursor in this work.

The results of this work are reported here, in which four bisdiazo compounds **1a-d** with electronically neutral (R = H), donating (R = Me) or withdrawing (R = NO_2) groups, along with

[a] *Oxford Suzhou Center for Advanced Research (OSCAR), Suzhou Industrial Park, Jiangsu 215123, P. R. China.*
[b] *Chemistry Research Laboratory, Department of Chemistry, University of Oxford, Oxford OX1 3TA, United Kingdom.*
[c] *JEOL (Beijing) Co. Ltd., Shanghai Branch, Shanghai 200335, P. R. China.*
*Corresponding author (*Email:*). mark.moloney@chem.ox.ac.uk
Supplementary Information available: [details of any supplementary information available should be included here]. See DOI: 10.1039/x0xx00000x

R = NH_2 which is known to both insert and crosslink giving polymeric material which has not been fully chemically characterised[15], were selected for study (**Scheme 1**). Then, a key question requiring an answer was whether carbenes might act as a C1 monomer, and directly polymerize, or whether polymerization might involve the diazo system along or in combination with the carbene, with several possible coupling scenarios being illustrated in Figure 1a. The carbene might directly couple, leading to alkene or alkane formation, or might react with the diazo starting material to give azine links, or both, and this makes for a complicated possible polymerisation mechanism. Additionally, for certain potential applications, a unique outcome might be accomplished by thermally induced homopolymerization from the bisdiazo-NH_2 **1d** on a polyvinyl alcohol (PVA) surface when conducted with a minimized volume of liquid phase in the open-air atmosphere.

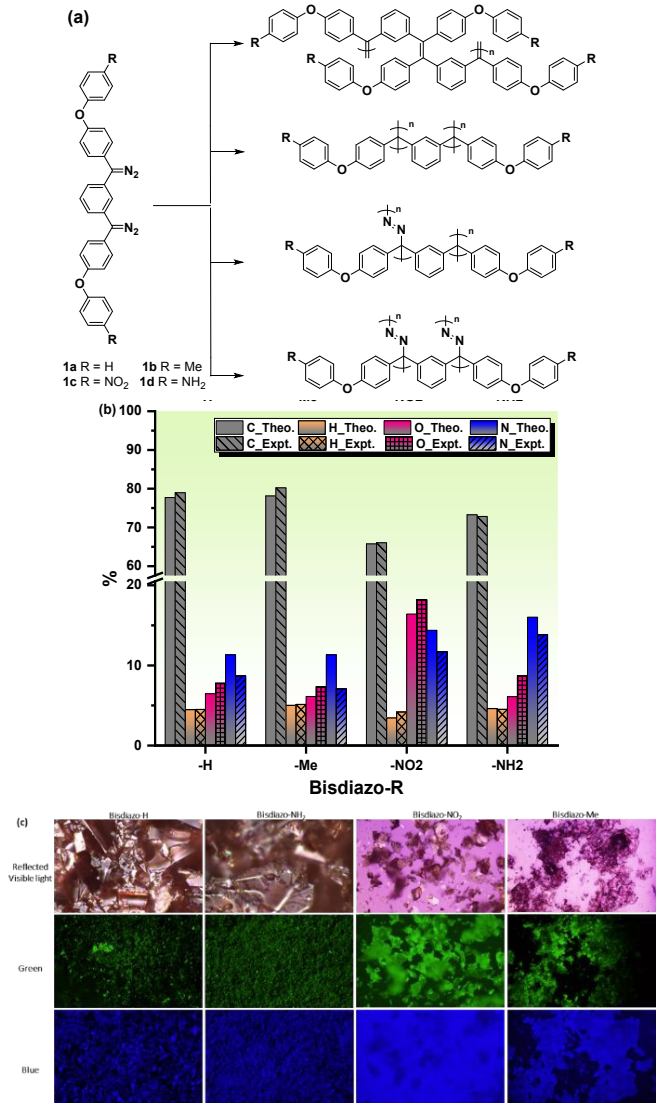

Figure 1. (a) Chemical structure of bisdiazo-R compounds **1a-d** and their possible repeat unit of polymers under catalyst-free polymerization, (b) elemental analysis and (c) optical and fluorescence images of bisdiazo-R compounds **1a-d** with varied terminal groups (R=H, Me, NO_2 and NH_2).

Results and discussion

Monomer synthesis. The required bisdiazo monomers with chemical structure shown in Figure 1a were readily prepared as shown in **Scheme S1-S3** using reported methods;[1, 16] thus, ethers **2a-d** were subject to Friedel-Crafts acylation with isophthaloyl chloride to give diketones **3a-d**. For **3a-c**, conversion to the corresponding bishydrazones **4a-c** and then oxidation to the bisdiazo species **1a-c** proceeded directly. In the case of ketone **2d**, reaction with hydrazine led to hydrazone formation along with hydrazinolysis of the amide, giving product **4d**, which upon oxidation gave bisdiazo **1d (Scheme S3)**. These were all purple-coloured solids, giving satisfactory element analysis (Figure 1b) and which also exhibit fluorescence when excited by green light of λ_{ex}=460-495 nm or blue of λ_{ex}=360-370 nm (Figure 1c).

Thermal properties of bisdiazo compounds. An initial study of bisdiazo compounds **1a**-**d** was made to understand thermal instability and identify the most suitable temperature range for decomposition. Thermal properties of bisdiazo compounds **1a-d** were evaluated by using Thermal Gravimetric Analysis (TGA) and Differential Scanning Calorimetry (DSC) as detailed in Figure S1. TGA showed weight loss of ~ 10 wt% as the temperature reaches 328°C (Figure S1a), which closely corresponds to the theoretical values of 11.32% and 10.68% for bisdiazo-H and bisdiazo-NH_2 terminal group after fully releasing dinitrogen (Figure S1e-S1f), consistent with initial collapse to the biscarbene. Noteworthy is that bisdiazo-NH_2 **1d** reacted significantly more rapidly than the other three compounds, and N_2 release upon heating continuously occurred over the temperature range up to 328°C for all bisdiazo compounds, rather than in one simple step (TGA traces in Figure S1a). The N_2 release rate with temperature increase was studied by Derivative Thermogravimetric (DTG) analysis (Figure S1b), showing that the compounds are relatively stable at temperatures up to ~220°C and that, with a heating rate of 5°C/min, the release of N_2 took at least 40 min.

DSC, on the other hand, was used to establish their thermal properties, i.e. a suitable temperature range for release of N_2 upon heating. The DSC trace of bisdiazo-NH_2 (Figure S1c) shows a relatively sharp endothermic peak around 50.5˚C, which is the expected glass transition T_g. By contrast, T_g is even clearer for bisdiazo-H at 27.2˚C (Figure S1c) showing a step-like transition. Those T_g points are very likely to be mislabelled as melting points solely based upon observation by naked eye.[1, 16] A similar pattern in T_g is also observed in DSC traces of bisdiazo-Me and bisdiazo-NO_2 exhibiting a step-like and sharp endothermic peak (Figure S1d), respectively.

For all the bisdiazo compounds, decomposition leading to release of N_2 commences by 110-112˚C, but with some variation depending on the identity of the terminal groups (Figure S1c-S1d), and in which the decomposition peak is broader for bisdiazo-NH_2 than for bisdiazo-H (Figure S1c). Thus, it seems that the identity of the terminal group is an important determinant for stability and decomposition. The combined data from Figure S1a-S1d implied that later mass spectra

View Article Online
DOI: 10.1039/D4PY01474J

analyses would need to be run at lower than 60˚C to see the necessary molecular ion, that other fragments would be observed at a higher temperature from 80 to 250˚C, and that bisdiazo compounds would only be fully decomposed higher than 600˚C.

To understand why the broadness of a decomposition peak in the DSC traces (Figure S1c-S1d) differs for each of the compounds, a stepwise isothermal DSC was carried out (Figure 2a-2c, Figure S1g). The release of N_2 started at about 60˚C for all the bisdiazo compounds, which is more significant for bisdiazo-NH_2 as compared to the other three (Figure 2a-2c), and lower in area for both the bisdiazo-Me and -NO_2 compounds (Figure 2b and Figure S1g), consistent with difference in activation energy. There are two major peaks for the release of N_2 for bisdiazo-NH_2 occurring at about 80˚C and 100˚C (Figure 2c), respectively, while only one exists at around 100˚C and is relatively sharp for bisdiazo-H at 80°C (Figure 2a), but broad at 80°C for bisdiazo-Me and -NO_2 (Figure 2b and Figure S1g), implying that other different terminal groups could be used to further adjust the thermal stability of this class of compound. In addition, even at the same temperature of 100˚C, being heated for 30 min does not release all the possible N_2 molecules in all the bisdiazo compounds, since there are further sharp peaks at higher temperatures of 120˚C and at 140˚C, especially noticeable for bisdiazo-NH_2 (Figure 2c).

Thermally induced catalyst-free solid-phase self-polymerization. From the visual appearance of the above thermal reactions, it was suspected that homopolymerization might be occurring in the molten phase of all the compounds (Figure S2a-S2b), and yellow-brown solids could be obtained after heating bisdiazo-H **1a** and bisdiazo-NH_2 **1d** at 90˚C for up to 3 hr in air, conditions chosen to simulate the TGA and DSC measurements under nitrogen (Figure S1a-S1d). The reaction products were only soluble in tetrahydrofuran (THF, Figure 2d), but not methanol, ethanol or acetone (Figure S2c). It was also noted that the product obtained was very viscous, adhering to glassware analogously to the reported surface modification of such bisdiazo compounds onto varied materials.[1, 2, 17]

Homopolymerization under air and nitrogen atmosphere under a vacuum up to 0.001 mbar was conducted and this gave a color change of the bisdiazo from purple-red before to yellow, after polymerization (Figure 2d)[18], while a foam-like structure was formed from solid phase self-polymerization at 120 °C for 3 hr under nitrogen atmospheric conditions (Figure 2e) which does not occur in the open air (Figure S2a). This is consistent with polymerization along with entrapment of the released N_2 gas in the newly formed polymer matrix. Molecular weight (MW) distribution measurement by Gel Permeation Chromatography (GPC, Figure 2f and Figure S3a) indicated a range peaking at about 2- 20 *kDa*, and the UV-vis spectrum (Figure 2g) further confirmed that a major peak of wavelength ~ 291 nm is reduced after polymerization while a broad shoulder arose at 320-380 nm, and complete disappearance of the diazo signal around 2020 cm^{-1} by IR measurement was observed (Figure S3b). For a typical monomer MW of *ca.* 500, this would correspond to the formation of oligomers of length 6 < n < 20. It was found that this process could be affected by both the temperature and atmospheric gas, especially oxygen (Table S1). Overall, the MW distribution is in the range of 1-10 *kDa* (Figure **2d**) with a polydispersity distribution *PDI* (*PDI=Mn/Mw*) of 2.04 to 2.75 (Table S1), regardless of the conditions applied, for bisdiazo-H **1a**. This looks like a step-growth polymerization mechanism and these values are close to polymers generated from diazo compounds mediated by catalyst.[19, 20] Importantly, this polymerisation occurred in the absence of catalyst in both air and an inert atmosphere like N_2.

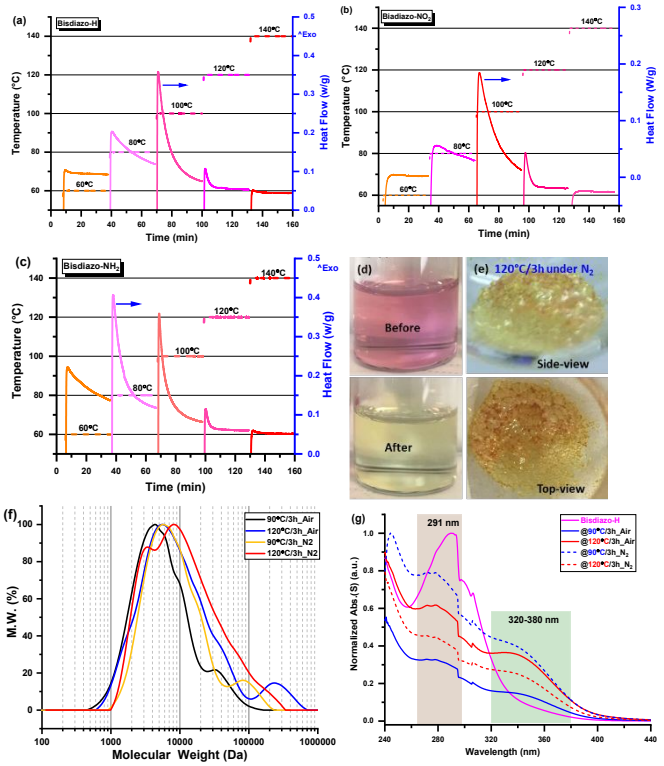

Figure 2. Stepwise isothermal DSC traces at various temperatures of (a) bisdiazo-H **1a**, (b) bisdiazo-NO_2 **1c** and (c) bisdiazo-NH_2 **1d**. (d) Color change of bisdiazo-H solution in THF before and after heating, (e) self-polymerization in nitrogen at 120˚C for 3h, (f) GPC traces of molecular weight distribution and (g) UV-Vis spectrum of self-polymerized bisdiazo-H **1a** under different conditions (in THF solution).

UV-Vis kinetic study of thermally induced catalyst-free liquid-phase self-polymerization. The thermal decomposition reaction time is expected to be around 24 hr at a lower temperature of 66˚C for bisdiazo compounds as indicated from the DSC and TGA data described above. Therefore, a THF solution of bisdiazo-NH_2 **1d** was used for a UV-Vis spectrum kinetic study as illustrated in Figure 3a, which were also carried out in organic solvents, namely toluene at 100°C (Figure 3b) and chlorobenzene at 120°C (Figure 3c) for a systematic study. The similar UV-Vis kinetic traces for the rest bisdiazo compounds **1a-c** in the combinations of solvents and temperatures are shown in Figure S4. For the compounds in THF solutions, the UV-Vis peak at ca. λ=295 nm (Figure 3a, Figure S4a-S4c) is ascribed to the diazo site

C=N=N, the intensity of which decreased with polymerization time. It also noted that there is a slight blue-shift for both starting bisdiazo-Me and bisdiazo-H compounds (Figure S4a-S4b), and a slight redshift for both bisdiazo-NH_2 and bisdiazo-NO_2 compounds (Figure S4c) in THF, consistent with the changing electronics of these systems. Furthermore, a minor peak at λ=250 nm increases in intensity during polymerization of bisdiazo-NH_2 **1d** (Figure 3a), which may be due to cross-linkage between the carbene and the terminal amine group (*vide infra*).

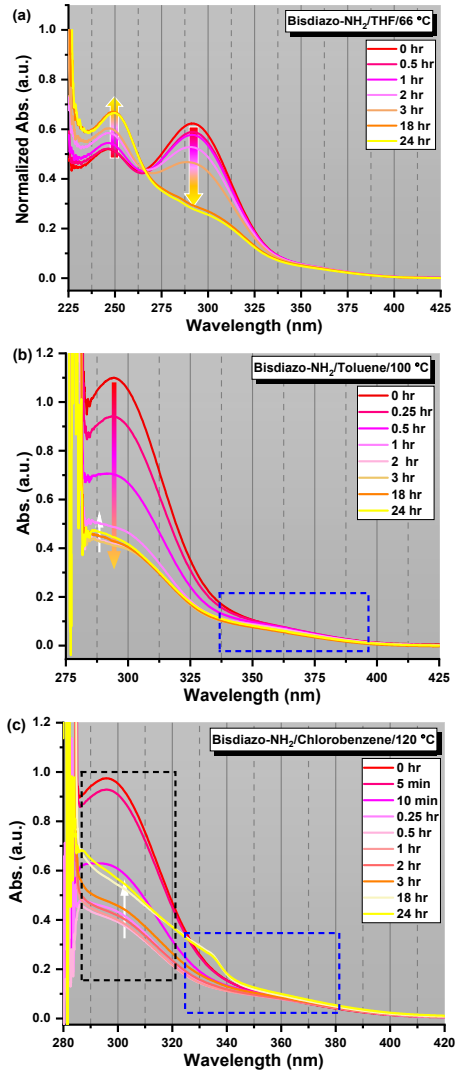

Figure 3. UV-Vis kinetic traces of bisdiazo-NH_2 compound polymerization in (a) THF as solvent at 66°C, (b) toluene at 100°C (b) chlorobenzene at 120°C (concentration=0.4 mg/mL). UV-Vis kinetic rate analysis: (d, e) kinetic observation of the polymerization of bisdiazo-NH_2 in different solvent-temperature combinations using Eq.(S11-S12).

In order to probe any temperature effect, UV-Vis kinetic studies were also carried out in another two organic solvents, namely toluene at 100°C and chlorobenzene at 120°C, the pattern of which from bisdiazo-NH_2 compounds are shown in Figure 4b-4c, and the others in Figure S4d-S4i. The most common observation is that the intensity of the major UV absorption peak ~295 nm decreased as polymerization proceeded, and a small noticeable shoulder ~ 345 nm developed at 10 min (blue dash-line boxed), although not so clearly for bisdiazo-NO_2 (Figure S4g-S4i).

The polymerization at 120°C went the most quickly as shown via both DSC and TGA traces (Figure S1a-S1d) in 10 and 15 min and could also be easily perceived from the fading colour of the reacting solution (Figure S9). A noticeable increase in intensity of the major UV absorption band at 295 nm as the reaction continues further after 0.5 and 1 hr, and a unique step-rise for bisdiazo-NH_2 after reaction for 18 hr and even longer (white-arrow in Figure 4b-4c) could be seen. A pattern (Figure S4d-S4i) of the major band at 290 nm and minor shoulder around 350 nm in the UV-Vis spectrum of all the bisdiazo compounds in the combinations of solvent-temperature was also observed as demonstrated in Figure S7, except for bisdiazo-NO_2 **1c**, and which is similar to polymerization of bisdiazo-Me in HPLC-grade DMSO-d6 polymerized at higher temperature of 120°C as shown in Figure S9c-S9d.

Figure S5 shows a simple kinetic analysis model which assumes decomposition of the diazo function directly to a carbene, and overall, this model works well for diazo R=H, Me and NO_2 compounds, but not for R=NH_2 which shows anomalous behaviour at elevated temperature. To study this difference more quantitatively, a consecutive reaction and/or polymerization was explored for the possible rate constants that involves polymerization of bisdiazo compound in varied solvent at different temperatures and demonstrated in Figure S6; this is more precise than the simplified one illustrated in Figure S5. The results from the simplified kinetic analysis in Figure S5 are acceptable for the polymerization carried out in THF at 66°C and in toluene at 100°C, but no fitted results could be obtained at the higher temperature of 120°C in chlorobenzene (gray-shaded area in Figure S6c), or even at 100°C in toluene for bisdiazo-NH_2 alone, which does not match the case described by Eq.(S10) or Eq.(S11) (Figure S6e). It also exhibits a solvent-temperature combination effect on the rate of constant calculation as portrayed in Figure S5e-S5f, described by the simplified Eq.(S1-S2), and such a solvent-temperature combination effect is also clearly supported by the UV-Vis spectrum observations of the resulting polymers as illustrated in Figure S7.

From the rate constant data as summarised in Table S3, there is a decrease in rate of carbene formation with increasing temperature along with activation for R= Me and deactivation for R = NO_2 as expected at all temperatures. In a number of cases, $k_1 = k_2$, and for polymerization in chlorobenzene (PhCl, 120°C), $k_2 > k_1$, so that the polymer is formed more effectively at higher temperature. While for those in THF at 66 °C or toluene (PhMe) at 100 °C, $k_2 < k_1$ or $k_2 = k_1$, so that even though the rate of formation of carbene is good, polymerisation is slower, since carbene does not react on as quickly.

View Article Online
DOI: 10.1039/D4PY01174J

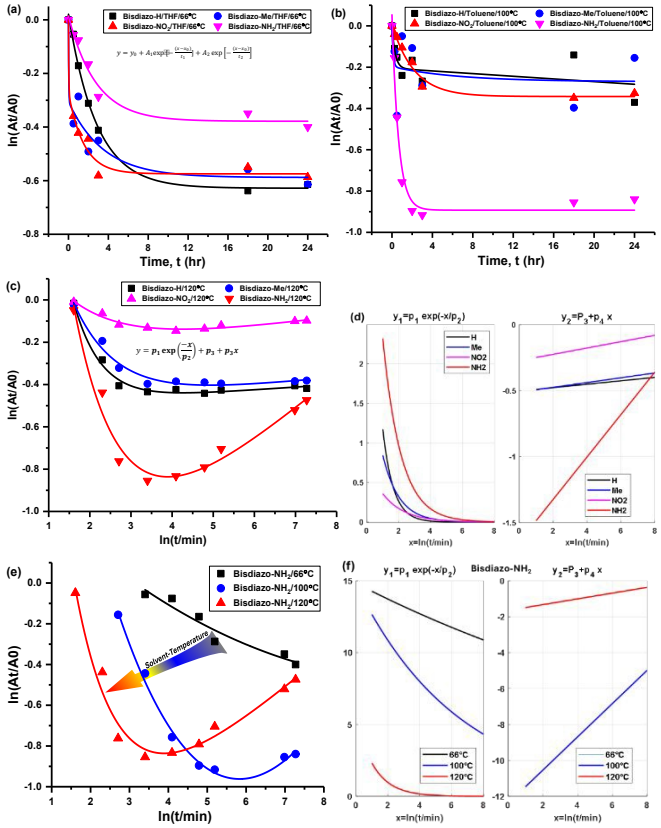

Figure 4. UV-Vis kinetic rate analysis: (a, b) a two-step consecutive polymerization for bisdiazo polymerization in THF at 66°C and toluene at 100°C described by Eq.(S10), (c, e) alternative description of polymerization in chlorobenzene at 120°C and (d, f) fitted kinetic contributions from both decomposed exponential and linear parts for the polymerization by Eq.(S11-S12), (e, f) kinetic observation of the polymerization of bisdiazo-NH_2 in different solvent-temperature combinations using Eq.(S11-S12).

Therefore, a two-step consecutive polymerization was considered (Figure S6a) and more details are given in Figure S6b. The corresponding findings are in Figure 4 and Table S2-S3 for the possible rate constants (i.e., k_1 for releasing nitrogen molecules and k_2 for further reaction of the diazocarbene or biscarbene intermediates) for each step as summed up in Table S2-S3. This analysis (Table S2-S3) suggests equal rate constants, k_1=k_2, for both R=H and R=NH_2 when polymerized in THF at 66°C, but $k_1 >> k_2$ for both R=Me and R=NO_2, suggesting that the second step of polymerization from the carbene species can become the rate determining step. Secondly, for the polymerization carried out in toluene at 100°C, $k_1 >> k_2$ for both R=H and R=Me, implying again that the second step is the determining step, while $k_1 = k_2$ applies for both R=NO_2 and R=NH_2 (Table S2-S3). More importantly, probing the rate constants for polymerization in chlorobenzene at 120°C is even more complicated than the two cases mentioned above and summarized in Figure 4c-4f and Figure S6c-S6d. In this scenario, both R=NO_2 and R=NH_2 coincidentally showed almost the same pattern (Figure S6c), while the polymerization process for both R=H and R=Me still fits the two-step consecutive reaction well enough, although an alternative Eq.(S11) fitting was successfully used for polymerization of all compounds at 120°C (Figure 4c). Such an alternative equation Eq.(S11) is more suitable for describing the scenario changes noticeable in the kinetics of polymer formation during the disappearance for each compound as exhibited in Figure 4d, especially for the polymerization of bisdiazo-NH_2 **1c** at higher temperatures of 100 and 120°C (Figure 4e-4f). Both Figures 4d and 4f show fitted kinetic contributions from both decomposed exponential and linear parts for polymerization. It looks like the exponential part (left sub-chart, Figure 4d) is more likely to be the production rate of carbene species or disappearance of diazo sites. The linear part (right sub-chart, Figure 4d) seems to be the rate of polymerization along with time, because it is almost the same trend for R=H, Me, NO_2 with the only difference coming from the terminal group R=NH_2, most likely due to significant electronic activation. In words, the rate of consumption of diazo sites is not necessarily equivalent to polymerization, and a two-step process, in which rate mismatch might occur, as seen in the polymerization of bisdiazo-NH_2 at higher temperatures (Figure 4e-4f), suggests that a solvent-temperature combination might be important in the outcome of polymerisation. Additionally, the contribution from the linear part for bisdiazo-NH_2 polymerization at lower temperature, i.e. at 66°C, is missing (right sub-chart, Figure 4f), implying that for heating at lower temperatures for bisdiazo-NH_2, the disappearance of diazo sites is the dominant one. Furthermore, the linear part in Figure 4f implies that crosslinking between the carbene centred carbon atoms with the terminal -NH_2 groups, and reaction at lower temperature, i.e. at 66°C, does not occur, but both the polymerization and crosslinking for reactions when carried out at both 100°C and 120°C does occur (Figure 4e). Such crosslinking between the carbene centred carbon atoms and the terminal groups would not be able to happen for the other three compounds (i.e., R=H, Me and NO_2) as manifested in Figure S6d-S6e. However, a plot of Hammett substituent constants[21] and the rate constants for the different combinations of temperature-solvent (Figure S6f) showed no direct correlation, underlying the complexity of the polymerisation sequence, especially so for 1d, where there are two reaction sites, at the carbene and amino centres.

Identity of polymer product. The UV-Vis spectra of the obtained polymers under varied solvent-temperature combination were studied to identify possible polymer linking groups (Figure S7), and several possibilities were identified (Figure 1a). There is a broad UV-Vis band at 285 nm for both polymers from R=H **1a** and R=Me **1b** with a shoulder at 350 nm (Figure S8), but which for R=NO_2 **1c** and R=NH_2 **1d** were closer to 295 nm. (Figure S8). This suggests the presence of different linking groups, and for R=H **1a** and R=Me **1b**, an azine linkage C=N-N=C is more likely, evidenced by a reported UV band of λ_{max} values at 275 nm,[22] while for R=NO_2 **1c**, a direct C=C linkage seems more likely to occur, evidenced by a reported λ_{max} value at 308 nm.[23] That such a difference would arise is not surprising, given different rates of collapse of diazo starting materials,

onward reaction and the stabilities of different intermediates, indicated by the values of k_1 and k_2 (Table S3). The terminal groups of the polymers could be diazo groups, stabilised within the matrix of the polymer, and which would be responsible for (weak) UV absorption.

Molecular weight and distribution analysis. The molecular weight (MW) and distribution traces obtained by GPC, of polymers derived from bisdiazo compounds **1a-d** reacted in several organic solvents and temperatures, shows at least a bimodal MW distribution in all cases (Figure 5), with DP higher for **1a**, **b** (R=H, Me) and lower for **1c, d** (R= NO_2 and NH_2). Increasing reaction temperature leads to higher MW for **1a**, **b**, but not for **1c, d** (R= NO_2 and NH_2), which are much less affected by temperature. This further supports the importance of the terminal substituent, and combination of solvent-temperature[24-27] for the reaction (see Figure S7). The specific MW distribution pattern of each type of bisdiazo compounds is significantly affected by its terminal group (especially MW subpeaks 1 and 2 in Figure 5a and 5b for electron neutral ones). In addition, each sub-MW peaks, labelled by circled numbers in Figure 5 and summarized in Table 1 for each bisdiazo compound, could be regarded as largely monodisperse with a *PDI* of about 1.03 ~ 1.19. Furthermore, it is noteworthy that the MW for all of the Peaks 3 is the least monodispersed (i.e. *PDI=Mw/Mn ~ 1.0 is for* monodisperse). Of interest is that R= NO_2 **1c** gives the cleanest polymer, characterise by one major peak in the GPC.

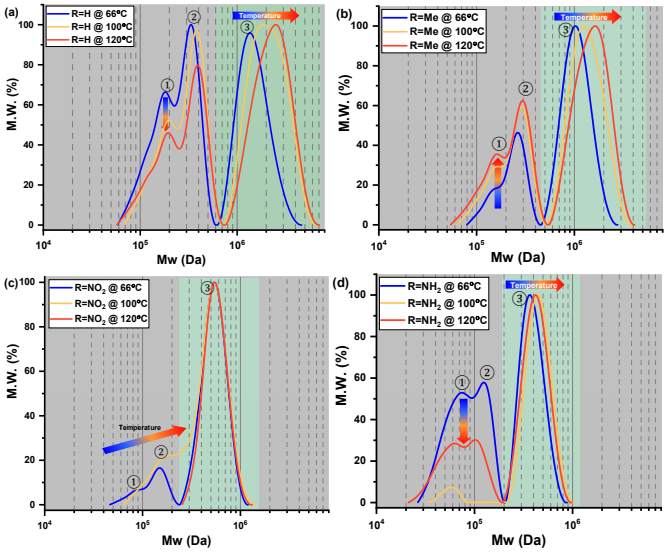

Figure 5. GPC obtained molecular weight (MW) distribution of bisdiazo-R polymerization in different solvent-temperature combinations for 24 h (a) R=H, (b) R=Me, (c) R=NO_2 and (d) R=NH_2.

Table 1. MW characteristics of bisdiazo-R polymerization in different solvent-temperature combinations (R=H, Me, NO_2 and NH_2).

Temp./°C	R=H Peak	Mn/kDa	*DP*	*PDI*	% Mn	R=Me Peak	Mn/kDa	*DP*	*PDI*	% Mn
66	①	68.43	138	1.10	32.85	①	65.84	126	1.03	9.86
	②	162.05	327	1.04	31.53	②	125.53	240	1.04	26.02
	③	**680.00**	**1375**	**1.13**	**35.62**	③	**491.49**	**940**	**1.10**	**64.12**
100	①	76.28	154	1.09	23.92	①	63.14	121	1.06	16.20
	②	182.66	369	1.05	30.33	②	136.82	262	1.05	27.09
	③	**920.53**	**1861**	**1.19**	**45.75**	③	**610.87**	**1169**	**1.14**	**56.71**
120	①	71.89	145	1.13	26.71	①	61.52	118	1.09	20.93
	②	188.66	381	1.05	27.00	②	141.63	271	1.04	25.64
	③	**1016.42**	**2055**	**1.18**	**46.29**	③	**676.21**	**1294**	**1.15**	**53.43**
Temp./°C	**R=NO_2 Peak**	**Mn/kDa**	***DP***	***PDI***	**% Mn**	**R= NH_2 Peak**	**Mn/kDa**	***DP***	***PDI***	**% Mn**
66	①	38.49	66	1.03	5.41	①	29.44	56	1.09	38.21
	②	71.25	122	1.03	12.72	②	62.93	120	1.03	21.06
	③	**253.76**	**434**	**1.08**	**81.87**	③	**184.59**	**352**	**1.07**	**40.73**
100	①	-	-	-	-	①	27.39	52	1.03	7.23
	②	71.906	123	1.10	23.52	②	-	-	-	-
	③	**241.400**	**413**	**1.11**	**76.48**	③	**212.32**	**405**	**1.08**	**92.77**
120	①	-	-	-	-	①	24.65	47	1.09	25.97
	②	-	-	-	-	②	53.05	101	1.04	16.98
	③	**262.69**	**449**	**1.08**	**100**	③	**198.16**	**378**	**1.08**	**57.05**

Note: *Mn* and *MW* stand for number and weight averaged molecular weight, respectively. DP is for the degree of polymerization. estimated by *Mn*/Bisdiazo-R. *PDI=Mw/Mn*.

Moreover, the MW dispersity (*PDI*) obtained in the three combinations of solvent-temperature relates to the kinetics (Figure 4). The lower MW distribution regions (MW Peaks 1 and 2) of all the polymers reflects the relative rate constants which control the MW distribution for the two-step consecutive polymerization, seen for both **1a, d** (R=H, NH_2) in THF at 66°C (Figure 5a and 5d, Table 1 and S2-S3), as well as both **1c, d** (R=NO_2, NH_2) in toluene at 100°C (Figure 5c-5d) with equal rate constants. At higher temperature of 120°C in chlorobenzene, a mismatch in kinetic rate as portrayed in Figure 4c-4f means that higher MW distribution dominates the resulting polymers as clearly illustrated in Figure 5d.

Here the MW, i.e. *Mn*, and degree of polymerization (*DP*) values are listed in Table 1, which are much better than those given in Figure 2d and Table S1, and this is likely to be a result of more effective liquid-phase polymerization for up to 24 hr for the former, as compared for only 3 hr for solid-phase polymerization for the latter. Secondly, for solid-phase polymerization, the honeycomb structure (Figure 2c and Figure S2) hindered further heat transfer needed for activating the

View Article Online
DOI: 10.1039/D4PY01474J

starting diazo compounds, giving a slower and longer reaction time, and overall, a less effective polymerization. In contrast, the liquid phase in varied solvents allows better maintenance of the set reaction temperature, allowing effective activation of the diazo sites to carbenes.

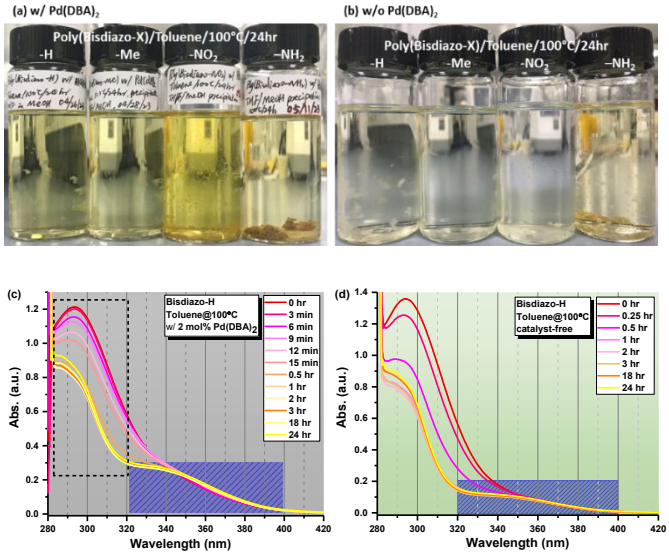

Figure 6. (a, b) Images and (c, d) UV-Vis kinetic spectra of polymer solutions in toluene at 100°C from thermally induced polymerization of bisdiazo-H compound (a, c) with (w/) and (b, d) without (w/o) (b, d) catalyst $Pd(DBA)_2$

Figure 6 sums up a comparison between the catalysed reaction process in the presence of palladium (II) (w/ in Figure 6a) and without using catalyst (i.e., w/o in Figure 6b) under similar reaction conditions. It turns out that polymer generated with Pd-catalyst is yellow (w/ in Figure 6a), and this might be due to the presence of nitrogen in the product or residual Pd-organic complex that usually could be removed by strong acid like hydrochloride acid.[28-30] Furthermore, the catalyst certainly enhances the polymerization as monitored by the UV-Vis spectrum (Figure 6c-6d), since a minor shoulder band in UV-Vis spectrum is more noticeable taking less time by using Pd-catalyst than that without (i.e., blue shaded box in Figure 6c-6d) for bisdiazo-H (others w/ Pd-catalyst are summarized in Table S4), indicating the reaction of bisdiazo systems upon heating may occur in a catalysed and uncatalyzed sense.

FD MS monitored self-oligomerization. To further analyse the self-polymerization behaviour of the bisdiazo compounds with different terminal groups, upon heating alone, high-resolution time-of-flight (HR TOF) MS system was used. The mass spectra of material generated by the self-polymerization of bisdiazo-R compounds in THF upon heating in vacuum, and the original FD chronogram with further analysed mass spectra are exhibited in Figure S10 and Table S5. Such field desorption (FD) chronogram (Figure S10a) confirmed the TGA data that showed the bisdiazo-NH_2 **1d** exhibited the highest decomposition temperature (Figure S1b). The exact mass of all the four starting bisdiazo compounds **1a-d** could be obtained with a lower capped current under two different current rates (Figure S11), which minimized the *m/z* peak of 662 at a higher current rate of 51.2 mA/min for bisdiazo-NH_2. Along with dimer and trimer products, other decomposition fragments were observed at elevated temperatures (Figure S10c-S10f).

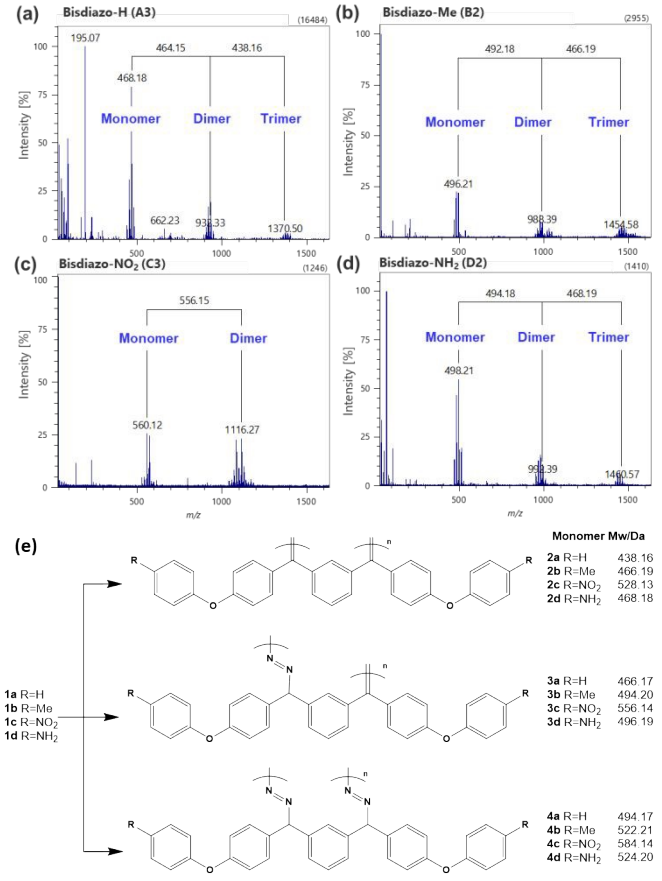

Figure 7. FD HR-TOF MS spectra of self-polymerized material upon heating under vacuum for (a) bisdiazo-H **1a**, and (b) bisdiazo-Me **1b**, (c) bisdiazo-NO_2 **1c** and (d) bisdiazo-NH_2 **1d** (e) possible repeating unit of oligomerization structures with monoisotopic *m/z*.

The mass spectra of all the four bisdiazo compounds **1a-d** upon heating in vacuum exhibits a cluster pattern as shown in Figure 7a-7d, clearly showing the monoisotopic *m/z* of dimer and trimer products except that for **1c** bisdiazo-NO_2 (Figure S10c-S10f). Specifically, the monoisotopic *m/z* for **1a** bisdiazo-H and **1d** bisdiazo-NH_2 (494.17 and 524.20, respectively) were easily observed (Figure S10c and S10f, and Figure S11a and S11d), representing the first mass spectrometric detection of diazo compounds that are normally too unstable for successful MS analysis. For both **1a** bisdiazo-H and **1d** bisdiazo-NH_2 compounds (Figure 7a and 7d), different fragments were observed at higher temperature before reaching final decomposition, and dimers and trimers could be seen in the mass spectra, but tetramer and higher oligomers were not since they are beyond the detection limit of *m/z* 1600. The existence of such dimers and trimers, even tetramers, further supports the occurrence of self-polymerization of those bisdiazo compounds to give structurally novel polymers without the need for catalysis. The possible structure of those oligomers, formed through the linkage of -C=N-N=C- or C=C is illustrated in

View Article Online DOI: 10.1039/D4PY01474J

Figure 7e. The varied combinations of those two linkers are the most probable reason for the cluster peaks for oligomerization and polymerization labelled as dimer and trimer in Figure 7a-7d.

Additionally, self-polymerization of bisdiazo-H and bisdiazo-NH_2 is different; while for the one with -H terminal group, stepwise-like polymerization, giving dimer and then trimer (Figure S10a and S10c, see corresponding A# regions in FD chronogram), while the other with -NH_2 terminal group exhibits dimer and trimer within the same time frame (Figure S10d, D# regions noted in FD chronogram). That difference could be due to changes in the carbene reactivity profile, or to the terminal group -NH_2 also reacting with the biscarbene, leading to possible rapid cross-linking[15] as shown in Figure 7e.

The predicted possible structures and *m/z* of the possible fragments, dimer and trimer of bisdiazo-H upon heating are shown in Figure S10g (based on the corresponding data of A# regions in FD chronogram, Figure S10c). This would be similar to the stepwise-polymerization of diazo compounds arising by transition-metal catalysed carbene cross-coupling,[31] so-called 'C1 polymerization'.[32] Similar C1 polymerization seems very likely for bisdiazo-H **1a** upon heating (Figure S4a and S4c), while in the case of bisdiazo-NH_2 **1d**, the presence of the terminal amine groups could lead to additional cross linking processes as discussed above.

Furthermore, instead of releasing both dinitrogen at the same time, such stepwise polymerization seems to proceed by releasing just one nitrogen at a time at lower temperature and possibly another dinitrogen at a higher temperature as exhibited in the dimerization and trimerization as noted in Figure 7a-7d, and illustrated in the TGA which clearly indicates a slow evolution of nitrogen as temperature is ramped. Here, a cluster for dimer with multiple *m/z* close to 14.00 equals to a nitrogen atom, and this matches the continuous weight loss as perceived by TGA (Figure S1b) and the fact that the accumulated weight loss rate is less than 10%wt even at 180˚C (Figure S1a). This is closer to the trend of releasing nitrogen with 30 min at varied temperatures (Figure 2b), and heating for just tens of seconds releases one nitrogen as the mass (*m/z*) difference of 28 was observed (A1 region in Figure S10c, and B1 region in Figure S10d. Similar predictions for bisdiazo-NH_2 **1d** compound are more complicated, since reaction at both carbene and amine groups is possible (Figure S10f and S10h); dimer and trimer fragments showed in mass spectrum in the very small-time frame as stated in Figure S10f and S10h (sub region D2). This difference is highly likely because of possible electronic modification of the terminal group.[33, 34] The patterns of dimer and trimer from mass spectrum is similar for all reactions, indicating homooligomerisation.

The possible monomer units of those oligomers, formed through the linkage of -C=N-N=C- or C=C is illustrated in Figure 7e, but analysis of the data in Figure 7a-7d clearly shows that the oligomer may be clearly formulated as **5** below for all values of R and for n=2, 3; this confirms the repeat unit to be C=C, and indicates that this reaction is a C1 polymerisation occurring under thermal and uncatalyzed conditions.

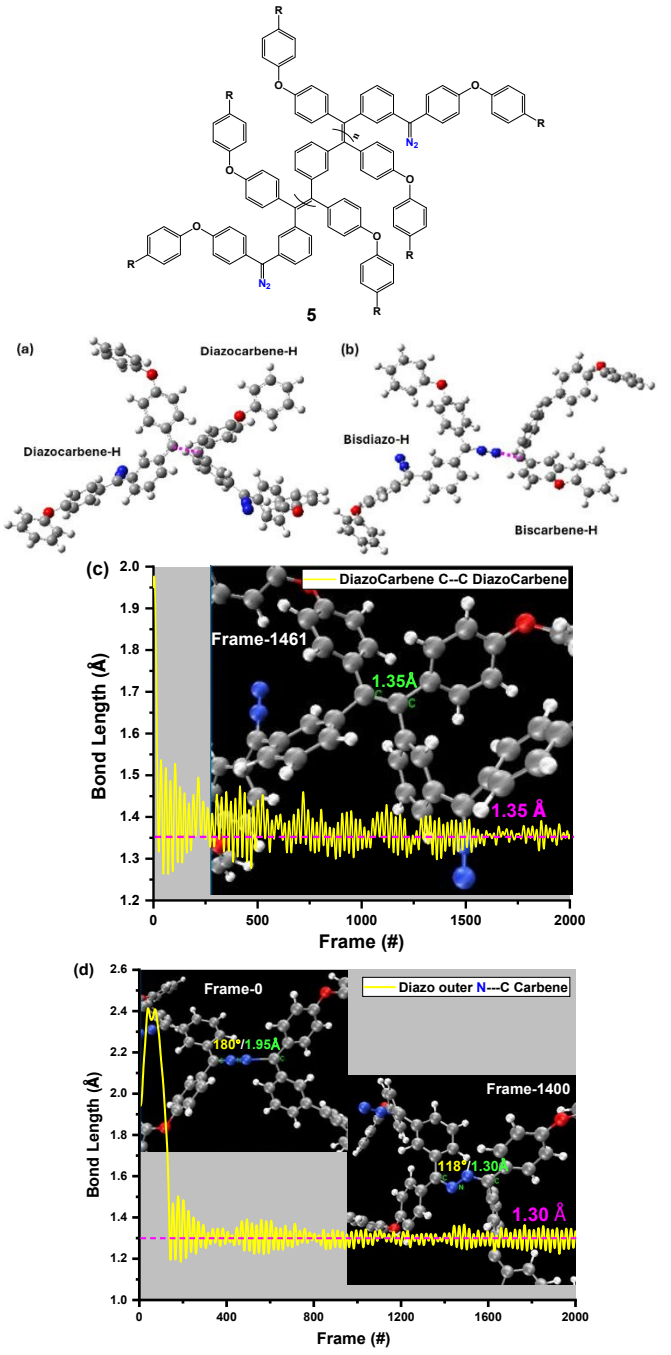

Figure 8. (a, b) Possible dimer structures for molecular dynamic (MD) calculations of (a) C---C bond formation from both carbene centered C atoms and (b) C=N-N---C bond from carbene centred C atom and N from a diazo site. (c, d) MD calculated bond length profiles of (c) C---C and (d) C=N-N---C bonds. (here using bisdiazo-H and its carbene species, i.e., diazocarbene-H and biscarbene-H; on the inset images of MD frame picked out, the purple dash-line for the possible bonds between atoms; green labels the bond length and yellow is the bond angle).

Molecular dynamics (MD) calculated bond length of the linkage in a dimer. To elucidate the fundamental aspects of all the bisdiazo compounds, the density functional theory (DFT) calculations were conducted and from the comparisons

between the calculated and experimental spectra (IR and UV-Vis in THF), and there is a good match for the IR (Figure S14) and also a very close one for the UV-Vis in THF (Figure S15). Similarly, the reacting carbene species leading to dimer formation involving an active singlet carbene species[35] have been modelled by carbene-carbene coupling or by carbene- diazo coupling (Figure 8a-8b). The C1 polymerization mentioned above grows polymer chains in single carbon increments[11, 36], as opposed to more usual 'C2 polymerisation' in the preparation of saturated main-chain carbon-based polymers. In the present work, linking C=C and -C=N-N=C- are possible. This assumption could be verified by molecular dynamic (MD) analysis (Figure 8c-8d), for which the bond length profiles are portrayed in Figure 8a-8b (purple dash line). As can be seen from Figure 8c, the calculated bond length of C---C from both carbene centred carbon atoms is around 1.35 *Å*, which is quite closely match to that of a typical sp^2-sp^2 C=C bond in length of 1.34 *Å*.

Similarly, the linkage of -C=N-N=C- from a diazo site and a carbene centred carbon atom could be confirmed with the calculated bond length of C---N about 1.30 *Å,* close to be a typical sp^2 C=N bond (Figure 8d), at the same time, the bond angle of C=N-N is reduced to around 110-130° from the previous 180° for the diazo site C=N=N. All these MD calculated values confirm that both linkers are feasible.

Self-polymerization induced nanostructure on polymeric surface. The biscarbene polymerization reported here works without any metal-based catalyst, and tolerates oxygen conditions, in both solid- phase and liquid-phase. Although diazo and similar bisdiazo compounds have been used for surface modification on various substrates,[1, 16] the molecular nature of these biscarbene modifications has not been determined, and the exact nature of surface modification becomes unclear. Besides the direct carbene insertion and/or cross linking[37] at the surface, carbene polymerization and polycondensation[38-40] can occur. To understand this further, the surface modification of bisdiazo-NH_2 on polyvinyl alcohol (PVA) was studied through the liquid-phase polymerization in open-air with a minimized volume of organic solvents; noticeable color changes were immediately observed as shown in Figure S12a, and full range X-ray photoelectron spectroscopy (XPS) is shown in Figure 9a.

This outcome would be consistent with self-polymerization of bisdiazo-NH_2 upon heating. After surface modification by bisdiazo-NH_2 compounds, regardless of solvent system, there are significant changes and carbons from the aromatic surface are clearly visible, as evidenced by small broad π-π* satellite peak[41] (Figure S13a), consistent with polymerization. The conjugated-like structure form is most likely derived from carbene self-polymerization, along with surface modification, and confirms the assumed possible polymerization and crosslinking from bisdiazo-NH_2 induced surface modifications[15]. Atomic force microscopy (AFM) using two-dimensional fast Fourier transform (2D FFT) images shows that the surface topography and phase changes significantly (Figure 9b). Furthermore, Figure 9c demonstrates the surface nanomechanical properties of the surface modified PVA thin film. As compared to the bare PVA thin film, the surface adhesion changed a little, but both stiffness and Derjaguin-Muller-Toporov (DMT) modulus almost doubled. This could be explained by the introduction of a molecular repeat unit, which is linear for PVA but full of aromatic rings for self-polymerized biscarbene that crosslink the PVA, giving a network which is more rigid.

The dynamic water contact angle (WCA) (Figure 9d-9e) of unmodified PVA thin film has water contact angle in the range of 75-90˚, holding water for up to 15 sec, although for times longer than 15 sec, water penetration occurs, as illustrated in the inset image in Figure 9d-9e. After surface modification using the bisdiazo-NH_2 compound, the water contact angle is quite stable with time and in the range of 75-90˚, which is close to the reported WCA of different diazo-based cross-linkers applied to ultrahigh molecular weight polyethylene[42]. This is likely for two reasons: the bisdiazo-NH_2 creates a heavily aromatic ring-based polymer-like thin film on the PVA surface upon heating at 120˚C for 1 hr, leading to a hydrophobic surface, and on the other hand, the polar nature of -NH_2 existing in such a polymer-like thin film, results in a hydrophilic surface. The cone-like nanostructures[43, 44] formed on the surface of PVA thin film (Figure 9b-9c), as a result of self-polymerized biscarbene, might also affect the dynamic WCA[43] as shown in Figure 9e, since the surface topology (Figure 9b) and nanomechanical properties (Figure 9c) are changed. This demonstrates that oxygen-tolerated surface functionalization may be achieved through a catalyst-free polymerization of biscarbene from the thermal decomposed bisdiazo compound simply by an open-air heating process with a minimized volume of liquid phase.

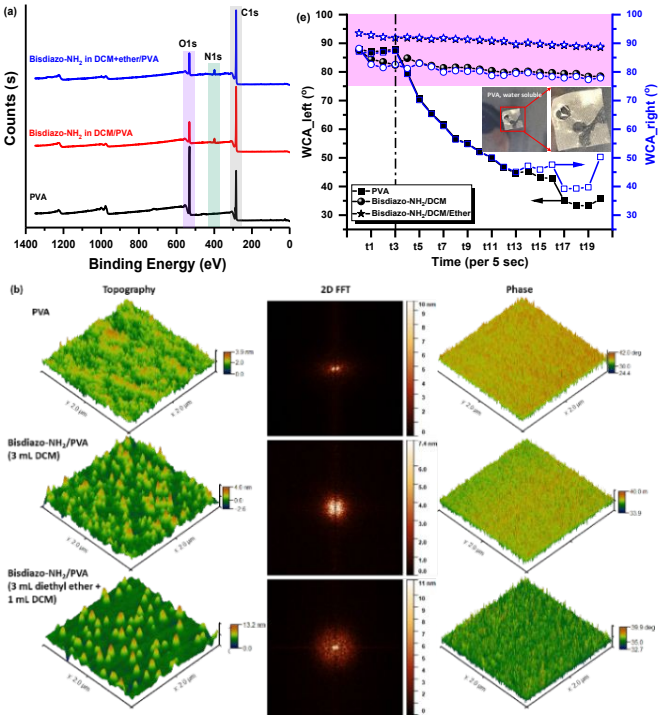

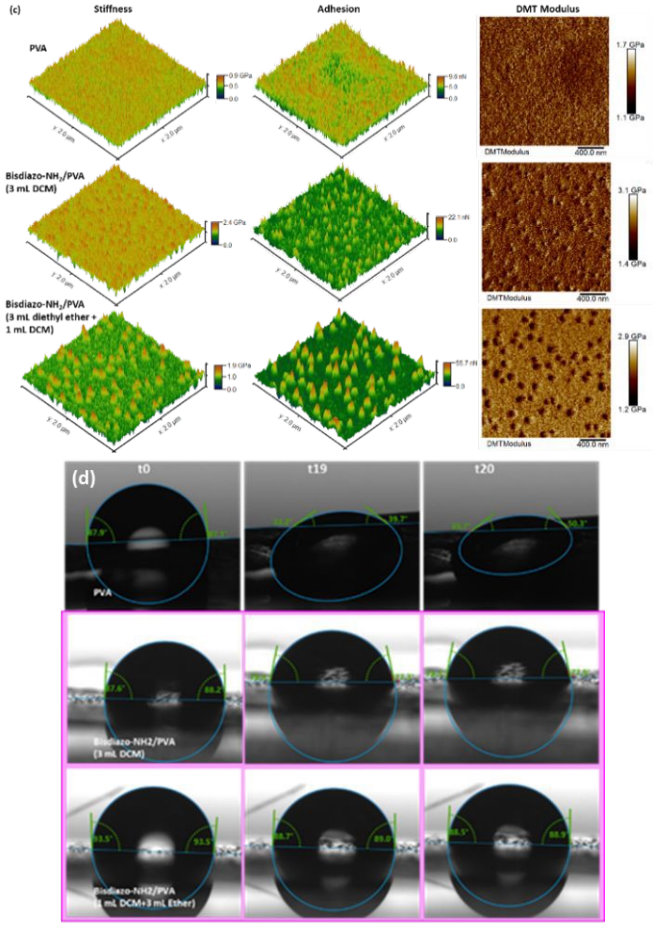

Figure 9. (a) Full range XPS scans, (b) AFM 2D FFT and phase images under tapping mode, (c) AFM-QNM results and (e) dynamic water contact angle (WCA) of PVA thin film before and after surface modification by using biadiazo-NH_2 in different solvent systems.

Experimental

Reagents, procedure and characterization for bisdiazo compounds

The bisdiazo compounds with varied terminal functional groups are illustrated in Figure 1a, and the reagents and procedure for synthesizing each one is detailed in Supporting Information Section 1.1 through 1.3 along with their structural characterization, including NMR and IR vibration measurements.

UV-Vis kinetic study of catalyst-free polymerization upon heating

A solution of bisdiazo compounds in organic solvents in HPLC-grade, such as THF, toluene and chlorobenzene, at a concentration of 0.4 *mg/mL* was explored for polymerization kinetic study at predetermined time intervals with sampling a reaction mixture of 100 µL. Using a solution diluted with 2.5 *mL* HPLC solvent in a quartz cuvette for UV-Vis absorption measurements (UV-1900, SHIMADZU, Japan) in range of 200-700 nm, scanning at intermediate rate and 0.2 *nm* data point collection at room temperature, were collected. In this UV-Vis kinetic study, the polymerization of bisdiazo compound was conducted at refluxing in THF at temperatures of 66 °C, 100 °C in toluene and 120 °C in chlorobenzene for 24 hr, respectively.

A similar UV-Vis kinetic study on Pd-mediated polymerization of bisdiazo-R compounds as a reference for the catalyst-free polymerization. Briefly, a mixture of 2.0 mol% based on bisdiazo-R compounds with the catalyst $Pd(DBA)_2$ (0. 4 mg, 0.80 µmol) in 50 *mL* of HPLC-grade toluene at 100°C in a round-bottom flask was stirred at 325 *rpm* for 30 sec at room temperature. Afterwards, 20 *mg* solid powder of bisdiazo-R compound was added and stirred for 30 sec at room temperature (RT). Then, the mixture was stirred in an oil-bath of 100°C for 24 hr. Sampling the liquid reaction mixture at the predetermined interval time for UV-Vis kinetic analysis and the kinetic observation is illustrated in Figure 6. After cooling to RT, the volatile materials were removed under reduced pressure, and the residue was dissolved in 5 *mL* HPCL-grade THF and precipitation in 15 *mL* HPLC-grade MeOH, which would be precipitated out as demonstrated in Figure 6a.

Molecular weight via Gel Permeation Chromatography (GPC)

Gel Permeation Chromatography (GPC) analysis of the self-polymerized materials from bisdiazo precursors was used to measure the molecular weights using a Shimadzu modular system comprising of a CBM-20A system controller, an SIL-20A automatic injector, a 10.0 *µm* beadsize guard column (50 × 7.5 *mm*) followed by column KF-803L and KF-802 in series (both 300 × 8 *mm*, Shodex™), an SPD-20A ultraviolet detector, and an RID-20A differential refractive-index detector. The temperature of the columns was maintained at 40 °C using a CTO-20A oven, and the eluent was THF (HPLC grade) for a sample concentration of 0.5 *mg/mL* with an LC-20AD pump running at isocratic flow mode at a rate of 1.0 *mL/min*. A molecular weight calibration curve was produced using commercial narrow molecular weight distribution polystyrene (PS) standards with molecular weights ranging from 1300 to 1.18×10^5 *Da*.

Homopolymerization monitored by FD HRMS

All the bisdiazo compounds were dissolved in THF (HPLC grade, 10 *mg/mL*), about 4 *µL* which was dropped on the direct insertion probe under Field Desorption mode (FD) by using a High-Resolution Time of Flight (HR-TOF) mass spectrometric system (JMS-T2000GC 'AccuTOF™ GC Alpha', JEOL, Japan). Ionization was then activated with a voltage of -10 kV and a current of 40 *mA*, and the ion source was at OFF mode with a temperature of 40˚C and the temperature of the probe was programmed with an increasing rate of 25.6 *mA/m* in from 0 up to 40 *mA*. As the probe reaches the current of about 40 *mA*, its corresponding temperature would be approximately 600˚C. The ion range (*m/z*) monitored by JMS-T2000GC 'AccuTOF™ GC Alpha' system is from 35 to 1600. The original FD chronograms and for mass spectrometric analysis are summarized in Figure S9 and Table S5 (SI), respectively.

Surface modification and characterization of PVA thin films

As-prepared PVA and its surface modified one are detailed in preparation and characterization in in Supporting Information Section 3, and characterization covered via Field Emission Scanning Electron (FE-SEM) Microscope for morphologies, X-ray photoelectron spectroscopy (XPS) for surface probing, and

Atomic Force Microscopy (AFM, Bruker Dimension Icon) for topography and phase images, etc.

Molecular dynamic (MD) analysis of linkers' formation

To get a further theoretical understanding of the possible linkers, i.e., C=C from both carbene centred carbon atoms and the -C=N-N=C- from a carbene centred carbon atom and nitrogen atom from the diazo site, the molecular dynamic (MD) calculation via using free quantum computational chemistry software ORCA 5.0.3[45] was explored using bisdiazo-H compounds and its carbene species as example for the possible dimers at the theoretical level of B97-3c with the default basis sets[46, 47] as detailed in Supporting Information Section 4. The MD input file was obtained with the help of another free multifunctional wavefunction analyser, Multiwfn version 3.8 (dev)[48], and the results were rendered by VMD 1.9.3 software[49] for analysing and extracting the bond length profile and angle measurements, with more details described in the SI file.

Conclusions

Overall, we report a detailed thermal evaluation of the decomposition of bisdiazo compounds substituted with various terminal groups. We have demonstrated that bisdiazo compounds thermally decompose at as low as 66 °C in the absence of catalyst for initiating a possible oligomerization, and even further polymerization at a higher temperature up to 120°C. It is also noted that such polymerization or reaction in the solid phase without any metal-catalysts gives foam-like products, consistent with loss of N_2, polymerisation and entrapment of the released gas in the polymer matrix, and the thermal properties and rates of reaction are affected by substituent terminal groups. From a further thorough UV-Vis kinetic technique, the reaction of nitrogen loss and catalyst-free polymerization proceeds in two steps with varied rate constants, depending on the nature of the terminal group and a combination of temperature-solvent. Both mass analysis and molecular dynamic calculations confirmed that the linking reaction is alkene formation, with diazo end groups. Importantly, the reaction is not only catalyst-free but also oxygen tolerant. Such catalyst-free oxygen-tolerant self-polymerization from biscarbene is a thermally induced reaction and can used for growth of unique nanostructure on polymeric substrates giving adjustment of surface properties. Such self-polymerization could generate a new family of polymers and mechanical characterization of these biscarbene-based polymers with different terminal groups is in progress.

Author contributions

Dr. Xiaosong Liu: Conceptualization, Synthesis, Methodology, All Measurements and Data curation, Formal analysis, density functional theory (DFT) and molecular dynamics (MD) calculations and results analysis, Writing, editing & reviewing-original draft. Prof./Dr. Mark G. Moloney: Conceptualization, Investigation, Supervision, Project administration, Writing- review & editing. Mr. Koji Okuda: Methodology and data curation on the FD HRMS monitoring bisdiazo compounds oligomerization, Writing- Review & editing.

Conflicts of interest

There are no conflicts to declare.

Data availability

The authors declare that the data supporting the findings of this study are available within the paper and its Supplementary Information files. Should any raw data files be needed in another format they are available from the corresponding author upon reasonable request.

Acknowledgements

This work was supported by Jiangsu Provencial Natural Science Foundation (General project, Grant Number BK20231223).

Notes and references

(1) Yang, P.; Moloney, M. G. Surface modification of polymers with bis(arylcarbene)s from bis(aryldiazomethane)s: preparation, dyeing and characterization. *RSC Advances* **2016**, *6* (112), 111276-111290, 10.1039/C6RA24392D. DOI: 10.1039/C6RA24392D.

(2) Yang, P.; Wang, Y.; Lu, L.; Yu, X.; Liu, L. Surface hydrophobic modification of polyurethanes by diaryl carbene chemistry: Synthesis and characterization. *Applied Surface Science* **2018**, *435*, 346-351. DOI: https://doi.org/10.1016/j.apsusc.2017.11.121.

(3) Harada, S.; Tanikawa, K.; Homma, H.; Sakai, C.; Ito, T.; Nemoto, T. J. C. A. E. J. Silver‐Catalyzed Asymmetric Insertion into Phenolic O–H Bonds using Aryl Diazoacetates and Theoretical Mechanistic Studies. *Chem. Eur. J.* **2019**, *25* (52), 12058-12062.

(4) Davies, H. M. L.; Liao, K. Dirhodium tetracarboxylates as catalysts for selective intermolecular C–H functionalization. *Nature Reviews Chemistry* **2019**, *3* (6), 347-360. DOI: 10.1038/s41570-019-0099-x.

(5) Wang, D.; Szabó, K. J. Copper-Catalyzed, Stereoselective Cross-Coupling of Cyclic Allyl Boronic Acids with α-Diazoketones. *Organic Letters* **2017**, *19* (7), 1622-1625. DOI: 10.1021/acs.orglett.7b00433.

(6) Allcock, H. R.; Hymer, W. C.; Austin, P. E. Diazo coupling of catecholamines with poly(organophosphazenes). *Macromolecules* **1983**, *16* (9), 1401-1406. DOI: 10.1021/ma00243a001.

(7) Chng, S.; Parker, E. M.; Griffiths, J.-P.; Moloney, M. G.; Wu, L. Y. L. A study of diazonium couplings with aromatic nucleophiles both in solution and on a polymer surface. *Applied Surface Science* **2017**, *401*, 181-189. DOI: https://doi.org/10.1016/j.apsusc.2017.01.017.

(8) Davis, P. J.; Harris, L.; Karim, A.; Thompson, A. L.; Gilpin, M.; Moloney, M. G.; Pound, M. J.; Thompson, C. Substituted diaryldiazomethanes and diazofluorenes: structure, reactivity and stability. *Tetrahedron Letters* **2011**, *52* (14), 1553-1556. DOI: https://doi.org/10.1016/j.tetlet.2011.01.116.

(9) Yu, X.; Yang, P.; Moloney, M. G.; Wang, L.; Xu, J.; Wang, Y.; Liu, L.; Pan, Y. Electrospun Gelatin Membrane Cross-Linked by a Bis(diarylcarbene) for Oil/Water Separation: A New Strategy To Prepare Porous Organic Polymers. *ACS Omega* **2018**, *3* (4), 3928-3935. DOI: 10.1021/acsomega.8b00162.

(10) Iqbal, S.; Lui, Y.; Moloney, J. G.; Parker, E. M.; Suh, M.; Foord, J. S.; Moloney, M. G. A comparative study of diaryl carbene insertion reactions at polymer surfaces. *Applied Surface Science* **2019**, *465*, 754-762. DOI: https://doi.org/10.1016/j.apsusc.2018.09.182.

(11) Jellema, E.; Jongerius, A. L.; Reek, J. N. H.; de Bruin, B. C1 polymerisation and related C–C bond forming 'carbene insertion' reactions. *Chemical Society Reviews* **2010**, *39* (5), 1706-1723, 10.1039/B911333A. DOI: 10.1039/B911333A.

(12) Cahoon, C. R.; Goossens, K.; Bielawski, C. W. Poly(carbyne)s via reductive C1 polymerization. *Polymer International* **2021**, *70* (1), 34-40. DOI: https://doi.org/10.1002/pi.6115 (acccessed 2025/03/12).

(13) Kang, S.; Lu, S. J.; Cho, M.; Cho, Y.; Sultane, P. R.; Bielawski, C. W. N-heterocyclic carbene copper complexes catalyze the C1 polymerization of substituted diazomethanes. *Journal of Polymer Science* **2024**, *62* (24), 5553-5561. DOI: https://doi.org/10.1002/pol.20240591 (acccessed 2025/03/12).

(14) Ihara, E. Development of polymer syntheses using diazocarbonyl compounds as monomers. *Polymer Journal* **2025**, *57* (1), 1-23. DOI: 10.1038/s41428-024-00954-1.

(15) Wang, D.; Hartz, W. F.; Christensen, K. E.; Moloney, M. G. Surface modification of glass fiber membrane via insertion of a bis(diarylcarbene) assisted with polymerization and cross-linking reactions. *Surfaces and Interfaces* **2022**, *32*, 102155. DOI: https://doi.org/10.1016/j.surfin.2022.102155.

(16) Yang, P.; Moloney, M. G. Surface modification using crosslinking of diamine and a bis(diarylcarbene): synthesis, characterization, and antibacterial activity via binding hydrogen peroxide. *RSC Advances* **2017**, *7* (47), 29645-29655, 10.1039/C7RA05258H. DOI: 10.1039/C7RA05258H.

(17) Mix, K. A.; Aronoff, M. R.; Raines, R. T. Diazo Compounds: Versatile Tools for Chemical Biology. *ACS Chemical Biology* **2016**, *11* (12), 3233-3244. DOI: 10.1021/acschembio.6b00810.

(18) Tian, R.; Ren, X.; Niu, P.; Yang, L.; Sun, A.; Li, Y.; Liu, X.; Wei, L. Development of chromenoquinoline-fused coumarin dyes and their application in bioimaging. *Dyes and Pigments* **2022**, *205*, 110530. DOI: https://doi.org/10.1016/j.dyepig.2022.110530.

(19) Wang, J. Diazo compounds: Recent applications in synthetic organic chemistry and beyond. *Tetrahedron Letters* **2022**, *108*, 154135. DOI: https://doi.org/10.1016/j.tetlet.2022.154135.

(20) Zhou, Q.; Gao, Y.; Xiao, Y.; Yu, L.; Fu, Z.; Li, Z.; Wang, J. Palladium-catalyzed carbene coupling of N-tosylhydrazones and arylbromides to synthesize cross-conjugated polymers. *Polymer Chemistry* **2019**, *10* (5), 569-573, 10.1039/C8PY01529E. DOI: 10.1039/C8PY01529E.

(21) McDaniel, D. H.; Brown, H. C. An Extended Table of Hammett Substitutent Constants Based on the Ionization of Substituted Benzoic Acids. *The Journal of Organic Chemistry* **1958**, *23* (3), 420-427. DOI: 10.1021/jo01097a026.

(22) Ferguson, L. N.; Goodwin, T. C. Absorption Spectra of Azines and Dianils. *Journal of the American Chemical Society* **1949**, *71* (2), 633-637. DOI: 10.1021/ja01170a069.

(23) Fang, Z.; Wu, F.; Tao, Q.; Qin, Q.; Au, C.; Li, Y.; Zhang, H.; Wang, N.; Yi, B. Substituent effects on the ultraviolet absorption properties of stilbene compounds-Models for molecular cores of absorbents. *Spectrochimica Acta Part A: Molecular and Biomolecular Spectroscopy* **2019**, *215*, 9-14. DOI: https://doi.org/10.1016/j.saa.2019.02.072.

(24) Sipos, L.; De, P.; Faust, R. Effect of Temperature, Solvent Polarity, and Nature of Lewis Acid on the Rate Constants in the Carbocationic Polymerization of Isobutylene. *Macromolecules* **2003**, *36* (22), 8282-8290. DOI: 10.1021/ma034581z.

(25) Cais, R. E.; Brown, W. L. Stereoconfigurations of Poly(vinyl bromide) and Poly(vinyl chloride). An Examination by Carbon-13 NMR of the Effects of Temperature and n-Butyraldehyde. *Macromolecules* **1980**, *13* (4), 801-806. DOI: 10.1021/ma60076a006.

(26) Krstina, J.; Moad, G.; Solomon, D. H. Effects of solvent on model copolymerization reactions. A 13C-NMR study. *European Polymer Journal* **1992**, *28* (3), 275-282. DOI: https://doi.org/10.1016/0014-3057(92)90189-9.

(27) Liu, B.; Wei, L.; Li, N.-n.; Wu, W.-P.; Miao, H.; Wang, Y.-Y.; Shi, Q.-Z. Solvent/Temperature and Dipyridyl Ligands Induced Diverse Coordination Polymers Based on 3-(2′,5′-Dicarboxylphenyl)pyridine. *Crystal Growth & Design* **2014**, *14* (3), 1110-1127. DOI: 10.1021/cg401599x.

(28) Ihara, E.; Hiraren, T.; Itoh, T.; Inoue, K. Palladium-mediated Polymerization of Diazoacetamides. *Polymer Journal* **2008**, *40* (11), 1094-1098. DOI: 10.1295/polymj.PJ2008145.

(29) Ihara, E.; Haida, N.; Iio, M.; Inoue, K. Palladium-Mediated Polymerization of Alkyl Diazoacetates To Afford Poly(alkoxycarbonylmethylene)s. First Synthesis of Polymethylenes Bearing Polar Substituents. *Macromolecules* **2003**, *36* (1), 36-41. DOI: 10.1021/ma021169v.

(30) Ihara, E.; Goto, Y.; Itoh, T.; Inoue, K. Palladium-Mediated Polymerization of Bifunctional Diazocarbonyl Compounds: Preparation of Crosslinked Polymers by Copolymerization of Bi- and Monofunctional Diazocarbonyl Compounds. *Polymer Journal* **2009**, *41* (12), 1117-1123. DOI: 10.1295/polymj.PJ2009065R.

(31) Xiao, Q.; Zhang, Y.; Wang, J. Diazo Compounds and N-Tosylhydrazones: Novel Cross-Coupling Partners in Transition-Metal-Catalyzed Reactions. *Accounts of Chemical Research* **2013**, *46* (2), 236-247. DOI: 10.1021/ar300101k.

(32) Jellema, E.; Jongerius, A. L.; Reek, J. N. H.; de Bruin, B. C1 polymerisation and related C-C bond forming 'carbeneinsertion' reactions reactions. *Chemical Society Reviews* **2010**, *39* (5), 1706-1723, 10.1039/B911333A. DOI: 10.1039/B911333A.

(33) Davies, H. M. L.; Denton, J. R. Application of donor/acceptor-carbenoids to the synthesis of natural products. *Chemical Society Reviews* **2009**, *38* (11), 3061-3071, 10.1039/B901170F. DOI: 10.1039/B901170F.

(34) Davies, H. M. L.; Morton, D. Guiding principles for site selective and stereoselective intermolecular C-H functionalization by donor/acceptor rhodium carbenes. *Chemical Society Reviews* **2011**, *40* (4), 1857-1869, 10.1039/C0CS00217H. DOI: 10.1039/C0CS00217H.

(35) Dobson, R. C.; Hayes, D. M.; Hoffmann, R. Potential surface for the insertion of singlet methylene into a carbon-hydrogen bond. *Journal of the American Chemical Society* **1971**, *93* (23), 6188-6192. DOI: 10.1021/ja00752a033.

(36) Cahoon, C. R.; Bielawski, C. W. Metal-promoted C1 polymerizations. *Coordination Chemistry Reviews* **2018**, *374*, 261-278. DOI: https://doi.org/10.1016/j.ccr.2018.06.017.

(37) Bourissou, D.; Guerret, O.; Gabbaï, F. P.; Bertrand, G. Stable Carbenes. *Chemical Reviews* **2000**, *100* (1), 39-92. DOI: 10.1021/cr940472u.

(38) Shimomoto, H. Synthesis of functional polymers by the Pd-mediated polymerization of diazoacetates and polycondensation of bis(diazocarbonyl) compounds. *Polymer Journal* **2020**, *52* (3), 269-277. DOI: 10.1038/s41428-019-0271-7.

(39) Shimomoto, H.; Mukai, H.; Bekku, H.; Itoh, T.; Ihara, E. Ru-Catalyzed Polycondensation of Dialkyl 1,4-Phenylenebis(diazoacetate) with Dianiline: Synthesis of Well-Defined Aromatic Polyamines Bearing an Alkoxycarbonyl Group at the Adjacent Carbon of Each Nitrogen in the Main Chain Framework. *Macromolecules* **2017**, *50* (23), 9233-9238. DOI: 10.1021/acs.macromol.7b01994.

View Article Online
DOI: 10.1039/D4PY01474J

(40) Wang, Y.-C.; Shao, Y.-J.; Liou, G.-S.; Nagao, S.; Makino, Y.; Akiyama, E.; Kato, M.; Shimomoto, H.; Ihara, E. Synthesis and electrochromic properties of polyamines containing a 4,4'-diaminotriphenylamine-N,N'-diyl unit in the polymer backbone: Ru-catalyzed N-H insertion polycondensation of 1,4-phenylenebis(diazoacetate) with 4,4'-diaminotriphenylamine derivatives. *Polymer Chemistry* **2022**, *13* (46), 6369-6376, 10.1039/D2PY01118B. DOI: 10.1039/D2PY01118B.
(41) Zhang, L.; Li, Z.; Tan, Y.; Lolli, G.; Sakulchaicharoen, N.; Requejo, F. G.; Mun, B. S.; Resasco, D. E. Influence of a Top Crust of Entangled Nanotubes on the Structure of Vertically Aligned Forests of Single-Walled Carbon Nanotubes. *Chemistry of Materials* **2006**, *18* (23), 5624-5629. DOI: 10.1021/cm061783b.
(42) Yang, S.; Yi, S.; Yun, J.; Li, N.; Jiang, Y.; Huang, Z.; Xu, C.; He, C.; Pan, X. Carbene-Mediated Polymer Cross-Linking with Diazo Compounds by C-H Activation and Insertion. *Macromolecules* **2022**, *55* (9), 3423-3429. DOI: 10.1021/acs.macromol.2c00527.
(43) Ambrosia, M. S.; Ha, M. Y.; Balachandar, S. The effect of pillar surface fraction and pillar height on contact angles using molecular dynamics. *Applied Surface Science* **2013**, *282*, 211-216. DOI: https://doi.org/10.1016/j.apsusc.2013.05.104.
(44) Yoo, M. J.; Ambrosia, M. S.; Kwon, T. W.; Jang, J.; Ha, M. Y. Wetting characteristics of a water droplet on solid surfaces with various pillar surface fractions under different conditions. *Journal of Mechanical Science and Technology* **2018**, *32* (4), 1593-1600. DOI: 10.1007/s12206-018-0314-6.
(45) U. Ekstrom, L. V., R. Bast, A. J. Thorvaldsen and K. Ruud. Arbitrary-Order Density Functional Response Theory from Automatic Differentiation. *J.Chem.Theor.Comp.* **2010**. DOI: DOI: 10.1021/ct100117s.
(46) Grimme, S.; Ehrlich, S.; Goerigk, L. Effect of the damping function in dispersion corrected density functional theory. *Journal of Computational Chemistry* **2011**, *32* (7), 1456-1465. DOI: https://doi.org/10.1002/jcc.21759 (acccessed 2025/03/03).
(47) Grimme, S.; Antony, J.; Ehrlich, S.; Krieg, H. A consistent and accurate ab initio parametrization of density functional dispersion correction (DFT-D) for the 94 elements H-Pu. *The Journal of Chemical Physics* **2010**, *132* (15), 154104. DOI: 10.1063/1.3382344 (acccessed 3/3/2025).
(48) Lu, T.; Chen, F. Multiwfn: A multifunctional wavefunction analyzer. *Journal of Computational Chemistry* **2012**, *33* (5), 580-592. DOI: https://doi.org/10.1002/jcc.22885 (acccessed 2025/03/03).
(49) Humphrey, W.; Dalke, A.; Schulten, K. VMD: Visual molecular dynamics. *Journal of Molecular Graphics* **1996**, *14* (1), 33-38. DOI: https://doi.org/10.1016/0263-7855(96)00018-5.

The authors declare that the data supporting the findings of this study are available within the paper and its Supplementary Information files. Should any raw data files be needed in another format they are available from the corresponding author upon reasonable request.

View Article Online
DOI: 10.1039/D4PY01474J